

# THE HISTRAP PROPOSAL: HEAVY ION STORAGE RING FOR ATOMIC PHYSICS\*

D. K. Olsen, G. D. Alton, S. Datz, P. F. Dittner, D. T. Dowling, D. L. Haynes, E. D. Hudson, J. W. Johnson, I. Y. Lee, R. S. Lord,\*\* C. A. Ludemann, J. A. Martin, J. B. McGrory, F. W. Meyer, P. D. Miller, W. T. Milner, S. W. Mosko, P. L. Pepmiller, and G. R. Young  
Physics Division, Oak Ridge National Laboratory, Oak Ridge, TN 37831

## Abstract

HISTRAP is a proposed synchrotron-cooling-storage ring optimized to accelerate, decelerate, and store beams of highly charged very-heavy ions at energies appropriate for advanced atomic physics research. The ring is designed to allow studies of electron-ion, photon-ion, ion-atom, and ion-ion interactions. An electron cooling system will provide ion beams with small angular divergence and energy spread for precision spectroscopic studies and also is necessary to allow the deceleration of heavy ions to low energies. HISTRAP will be injected with ions from either the existing Holifield Heavy Ion Research Facility 25-MV tandem accelerator or from a dedicated ECR source and 250 keV/nucleon RFQ linac. The ring will have a maximum bending power of 2.0 T·m and have a circumference of 46.8 m.

## Introduction

The success of the antiproton beam cooling work at the high-energy physics laboratories has greatly increased interest in synchrotron-cooler-storage rings for lower-energy atomic and nuclear physics studies. This interest has resulted in the ring projects at Aarhus,<sup>1</sup> Stockholm,<sup>2</sup> Heidelberg,<sup>3</sup> Tokyo,<sup>4</sup> and Darmstadt,<sup>5</sup> which are mostly for heavy-ion physics research. Other ring projects at Indiana,<sup>6</sup> Uppsala,<sup>7</sup> and Jülich<sup>8</sup> exist for light-ion physics research. HISTRAP, Heavy-Ion Storage Ring for Atomic Physics; is a proposed 2.0-T·m synchrotron-storage-cooler ring to be located at Oak Ridge National Laboratory (ORNL). HISTRAP will be injected with ions from either the existing Holifield Heavy Ion Research Facility (HHIRF) 25-MV tandem accelerator<sup>9</sup> or from a dedicated electron cyclotron resonance (ECR) source and 250 keV/nucleon radio frequency quadrupole (RFQ) linac.

The following desired capabilities for atomic physics research controlled the ring design: the need to accumulate, store, accelerate and decelerate highly charged very-heavy ions; the need for electron beam cooling to provide beams with extreme angular and energy resolution for precision spectroscopic studies; the need to study interactions between the circulating ion beam and internal fixed targets; the need to study interactions between extracted ion beams and external fixed targets; the need to study electron-ion interactions with circulating beams; the need to study photon-ion interactions with circulating beams; and the desire to store beams with multiple charge states separated by up to  $\pm 4\%$ . This charge state requirement is equivalent to a momentum acceptance of  $\pm 4\%$ .

The proposed HISTRAP facility shown in the lower left of Fig. 1 fulfills these needs. The ring has a circumference of 46.8 m and is designed for beams with magnetic rigidities between 0.1 and 2.0 T·m. The lattice, shown in Fig. 2, consists of four 90° achromatic bends connected by dispersionless straight sections. Each achromat consists of two 45° dipoles separated by a quadrupole triplet. The magnet aper-

tures were chosen for an injected-beam acceptance of  $40\pi$  mm·mrad in both the horizontal and vertical planes. The four long straight sections are each 4-m long. One straight section is required for the injection septum and the rf acceleration/deceleration cavity. Another straight section contains the electron beam cooling system. Eventually, another straight section will contain apparatus for a future resonant slow-extraction system to feed external beam lines. The last straight section has been kept completely free of accelerator hardware to allow space for apparatus to do in-ring experiments with stored ions.

## Lattice

A four-sided lattice was chosen because of space constraints. Because it is desirable to have injection, acceleration, extraction, cooling, and most internal experiments in dispersionless regions, all four 90° bends were chosen as achromats giving only dispersionless straight sections. The resulting lattice shown in Fig. 2 is four-fold symmetric and each achromat has reflection symmetry about its center. The achromats consist of two 45° dipoles separated by FDF quadrupole triplets. This lattice appears to minimize the number of quadrupoles, gives a small vertical  $\beta$  function in the dipoles, and gives a small dispersion function in the quadrupoles. The dispersion function must be small if more than one charge state is to circulate in the ring with reasonable quadrupole apertures. More complicated lattices seem to give no overall advantage. The horizontal and vertical tunes of the ring were chosen to be near 7/3, which avoids structure resonances and facilitates extraction by slow excitation of a sextupole resonance. In particular,  $\nu_x = 2.3088$  and  $\nu_y = 2.2744$  were used in the lattice calculations. The resulting  $\beta$  functions and the dispersion function are shown in Fig. 3. The lattice parameters are listed in Table 1.

A maximum dispersion function of 1.5 m occurs in the F quadrupoles. This dispersion corresponds to a displacement of  $\pm 6$  cm for cocirculating charge states separated by  $\pm 4\%$ . The maximum vertical  $\beta$  function occurs in the dipoles and is 5.7 m. In the straight sections the horizontal and vertical  $\beta$  functions are about 10 m and 5 m, respectively. About  $\beta \sim 10$  m gives an optimal cooling rate for ions with an energy of 50 MeV/nucleon, an emittance of  $40\pi$  mm·mrad, and an electron thermal temperature of 0.1 eV.

As listed in Table 1, the natural chromaticity of the lattice is given by  $\xi_x = -6.1$ . In order to have cocirculating charge states of the same species in the storage mode, it may prove necessary to cancel this chromaticity by using families of sextupole and higher order correction magnets. Since all the quadrupoles are in dispersive regions, this cancellation can be achieved locally as shown in Fig. 2 by placing a sextupole magnet next to each quadrupole magnet giving four sextupole families.

## Tandem Injection

The highest-charge-state beams for HISTRAP will be obtained with tandem injection. Table 2 summarizes the expected properties of tandem beams injected into HISTRAP. To calculate the number of injected ions per pulse or cycle in Table 2,  $N_{inj}$ , a source intensity of 200  $\mu$ A for the tandem was assumed. About half

\*Research sponsored by the U.S. Department of Energy under contract DE-AC05-OR21400 with Martin Marietta Energy Systems, Inc.

\*\*Consultant.

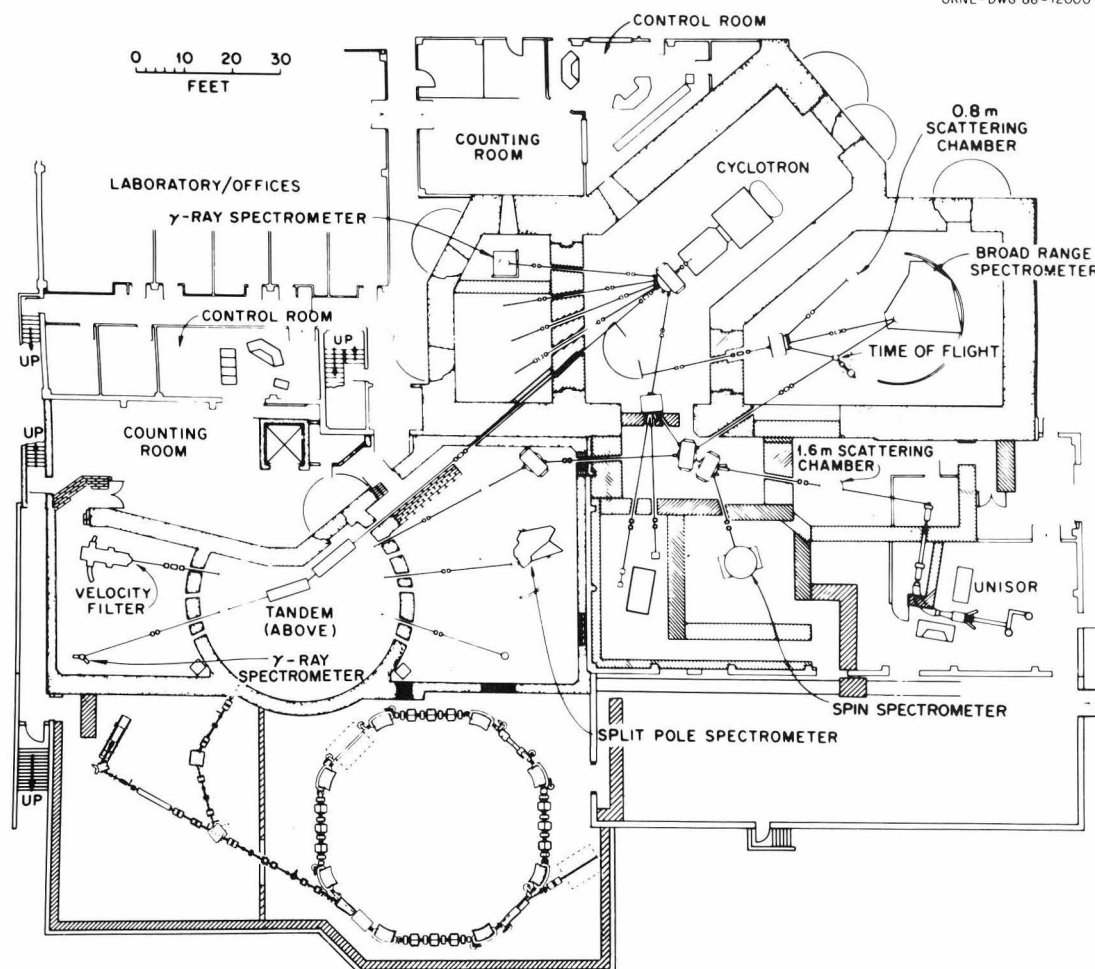


Fig. 1. Plan View of the proposed HISTRAP facility as an addition to the HHIRF. The storage ring in the lower left will be injected with ions from either the existing 25-MV tandem accelerator or from a dedicated ECR source and RFQ preaccelerator.

Table 1. Parameters of the Synchrotron Lattice  
Obtained from SYNCH Calculations

Magnetic rigidity	$B\rho = 2.0 \text{ Tm}$	
Circumference	$C = 46.7577 \text{ m}$	
Long straight (4)	$\ell_s = 4.0 \text{ m}$	
Dipole (8)	$\rho = 1.6666 \text{ m}$	
	$\theta = 45^\circ$	
	$\ell_D = 1.309 \text{ m}$	
Quadrupole (12)	$\ell_Q = 0.5 \text{ m}$	
$Q_F (8)$	$G_F = 3.6977 \text{ T/m}$	
$Q_D (4)$	$G_D = -4.1769 \text{ T/m}$	
Tune	$\nu_x = 2.3088$	$\nu_y = 2.2744$
Chromaticity	$\xi_x = -6.1846$	$\xi_y = -1.5242$
Beta function		
Dipole	$\hat{R}_x = 11.4 \text{ m}$	$\hat{R}_y = 5.7 \text{ m}$
Quadrupole	$\hat{R}_x = 12.2 \text{ m}$	$\hat{R}_y = 5.0 \text{ m}$
Straight	$\hat{R}_x = 10.5 \text{ m}$	$\hat{R}_y = 4.9 \text{ m}$
Dispersion function		
Dipole	$\hat{n}_x = 0.49 \text{ m}$	
Quadrupole	$\hat{n}_x = 1.51 \text{ m}$	
Straight	$\hat{n}_x = 0 \text{ m}$	

of this intensity level has recently been demonstrated with the tandem accelerator operating in a pulsed mode suitable for HISTRAP injection.<sup>10</sup> For these

tests an axial geometry cesium plasma sputter negative ion source was used.<sup>11</sup> In addition to the charge fractions from the two stripper foils, a transmission of 40% through the tandem was assumed, and a 20% loss was allowed for rf capture. Since the expected emittance of the beam from the tandem in a pulsed mode is about  $2\pi \text{ mm} \cdot \text{mrad}$  and the acceptance of the synchrotron is  $40\pi \text{ mm} \cdot \text{mrad}$ , it is believed that at least eight turns can be injected allowing a 40% filling of the synchrotron betatron phase space. The space-charge limit per pulse,  $N_{SC}$ , was calculated using a bunching factor of 50% and  $\Delta v = 0.08$ . The Keil-Schnell limit per pulse,  $N_{KS}$ , was calculated using  $\Delta P/P$  values resulting from straggling in a  $200\text{-}\mu\text{g}/\text{cm}^2$  carbon stripping foil. The number of injected ions corresponds to a time averaged current of 0.3 pA for light ions and 0.03 pA for very heavy ions. Figure 4 shows the maximum energy for these ions in HISTRAP. Light ions with  $Q/A = 1/2$  will be accelerated to 48 MeV/nucleon, whereas the very-heavy ions will be accelerated to about 7 MeV/nucleon.

Injection into HISTRAP from the tandem accelerator will require rotation of the existing  $90^\circ$  energy-analyzer magnet to the new transfer line shown in Fig. 1. The energy-analyzer magnet produces a double waist at which image slits control the tandem voltage and hence beam energy. The 23-m long transfer line is divided into three sections: a stripping section, an achromatic section, and a matching section. The



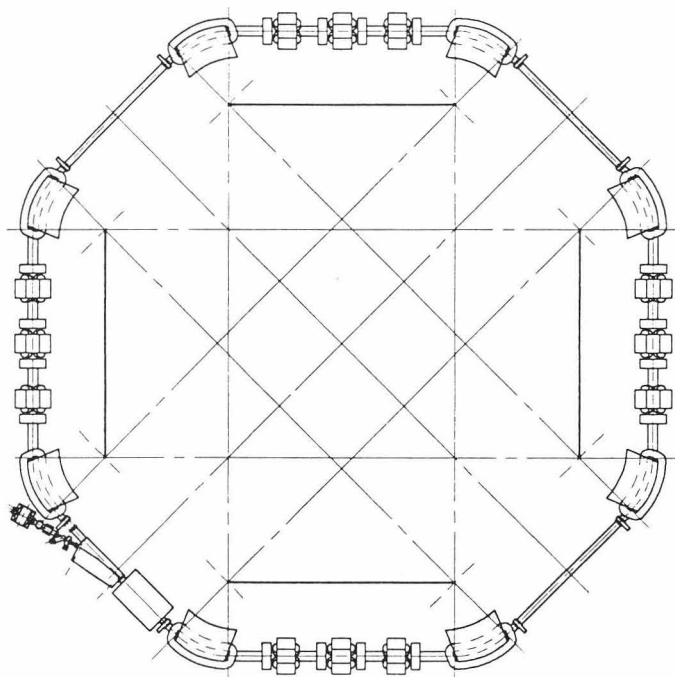


Fig. 2. The synchrotron-cooler-storage ring consists of four 4-m-long straight sections connected by 90° achromatic bends. Each achromat consists of two 45° dipoles separated by a quadrupole triplet.

foil at the double waist interfacing the stripping and achromatic sections will strip the ions to the charge states listed in Table 2. Slits in the center of the achromat, dispersion = 1.5 m, will select the desired charge-state for injection. The aperture at the double waist interfacing the achromatic and matching sections will separate the  $10^{-9}$  Torr tandem accelerator and transfer line vacuum from the  $10^{-12}$  Torr HISTRAP vacuum. Multiturn injection will be achieved by using an orbit bump in the horizontal plane.

Table 2. Properties of Beams from Tandem at Injection

Beam	Charge	E/A (MeV/ nucleon)	AP/P (%)	$N_{inj}$ ---	$N_{sc}$ (particles/pulse)---	$N_{ks}$ ---
$^{12}\text{C}$	6	4.0	0.058	$3.2 \cdot 10^9$	$1.3 \cdot 10^{10}$	$1.5 \cdot 10^9$
$^{16}\text{O}$	8	4.0	0.058	$1.3 \cdot 10^9$	$0.9 \cdot 10^{10}$	$1.2 \cdot 10^9$
$^{32}\text{S}$	15	7.6	0.031	$8.1 \cdot 10^8$	$1.0 \cdot 10^{10}$	$3.6 \cdot 10^8$
$^{40}\text{Ca}$	18	6.6	0.035	$6.3 \cdot 10^8$	$7.7 \cdot 10^9$	$3.4 \cdot 10^8$
$^{58}\text{Ni}$	24	5.3	0.042	$4.6 \cdot 10^8$	$5.1 \cdot 10^9$	$3.3 \cdot 10^8$
$^{79}\text{Br}$	27	3.9	0.053	$4.0 \cdot 10^8$	$4.0 \cdot 10^9$	$4.1 \cdot 10^8$
$^{127}\text{I}$	36	2.8	0.070	$3.3 \cdot 10^8$	$2.6 \cdot 10^9$	$4.6 \cdot 10^8$
$^{150}\text{Nd}$	38	2.4	0.079	$3.3 \cdot 10^8$	$2.3 \cdot 10^9$	$5.3 \cdot 10^8$
$^{197}\text{Au}$	40	1.9	0.098	$2.9 \cdot 10^8$	$2.2 \cdot 10^9$	$7.8 \cdot 10^8$

#### ECR-RFQ Injection

Since the HHIRF tandem accelerator is the primary instrument for the heavy-ion nuclear physics program at ORNL, its availability for HISTRAP injection will be limited. Consequently, a dedicated injector consisting of an ECR source and RFQ linac preaccelerator is included in the HISTRAP proposal. This second injector will produce 250 keV/nucleon beams with a lower charge-state than can be obtained from the

tandem accelerator. In addition, the number of ions per pulse which can be injected into HISTRAP with the ECR-RFQ source will be smaller than that with the tandem accelerator. The beam from the RFQ, as shown in Fig. 1, will be merged into the tandem transfer line before the common matching section.

The multicharged ion source will be almost identical to the ORNL ECR ion source which has been in operation since March 1984, reliably producing ion beams of a wide range of atomic species and charge-states.<sup>12</sup> Ions from the ECR source will be charge-state analyzed and transported to an RFQ linac. The conceptual design for this RFQ was developed in collaboration with the Lawrence Berkeley Laboratory group, which has successfully built two heavy-ion RFQ's.<sup>13</sup> Some parameters of this RFQ are listed in Table 3. It will accelerate ions with Q/A between 0.50 and 0.17 from 5 keV/nucleon to 250 keV/nucleon over a length of 2.4 m with a peak rf power input of 30 kW. The strongly diverging exit beam from the RFQ will be focused onto the entrance aperture of a debuncher located 110 cm down beam. This debuncher will be used to match the longitudinal emittance of the ion beam to the longitudinal acceptance of HISTRAP and is sized to reduce the momentum spread from about 1.0% to about 0.3%. The number of ions the ring will hold with injection with the RFQ is substantially less than listed in Table 2. The maximum acceleration energies for these ions in HISTRAP are also shown in

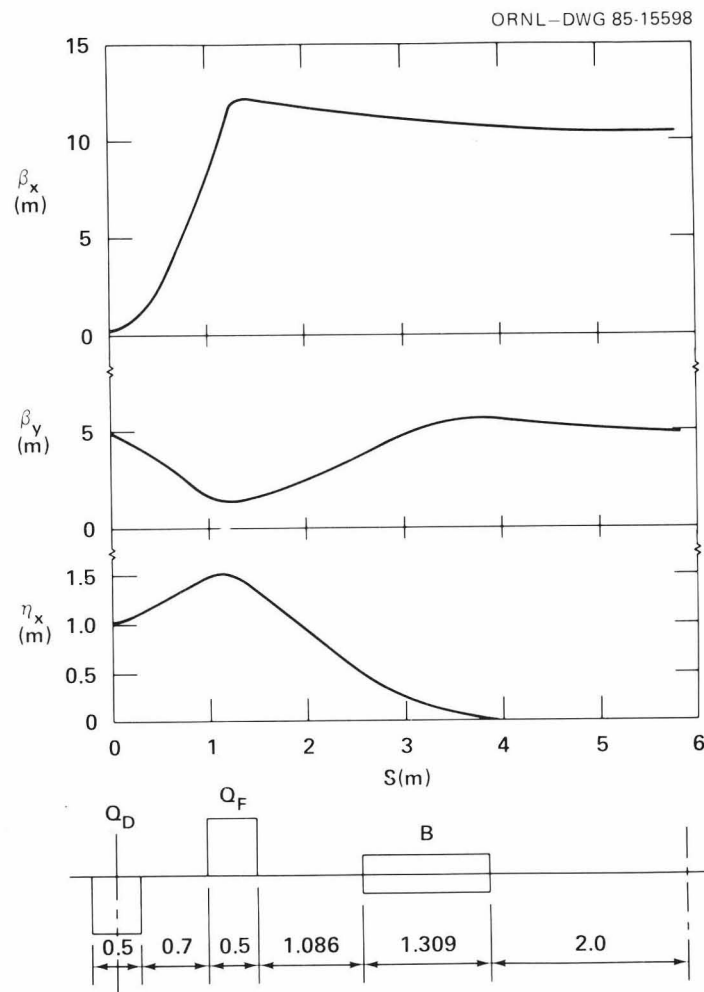


Fig. 3. Horizontal  $\beta_x$  and vertical  $\beta_y$  betatron functions and dispersion function  $\eta_x$  for one-eighth of the ring circumference. The ring has four-fold rotational symmetry and each quadrant has reflection-symmetry about the center of the defocussing quadrupoles.

Design ion	$^{197}\text{Au}^{+33}$
Frequency	228 MHz
Input energy	5 keV/nucleon
Output energy	251 keV/nucleon
Vane length	236.6 cm
Average bore radius ( $r_0$ )	1.42 mm
Maximum surface field	28 MV/m
Vane-vane voltage	29 kV
Peak rf power	30 kW
Cavity radius	13.7 cm

The most stringent quadrupole aperture requirement occurs for the F lens with the ring operating in the multiple-charge-state storage mode. In this mode it is assumed that three beams with  $\Delta Q/Q = -4\%, 0\%, +4\%$  must be stored and that each beam has  $\epsilon = 13\pi$  mm·mrad with  $\Delta P/P = \pm 0.10\%$ . Figure 5 shows the F

ORNL-DWG 85-17488

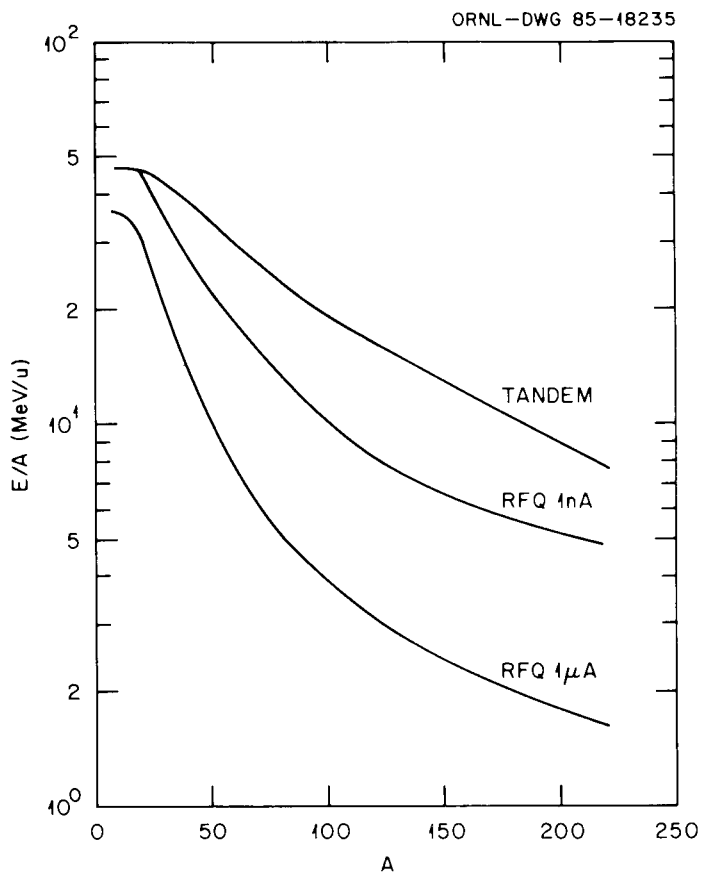


Fig. 4. Maximum ion energy from HISTRAP as a function of mass number with injection from either the tandem accelerator or injection from the ECR and RFO preaccelerator. For injection from the RFO two cases are shown: a high-charge-state low-current case (1 nA) and a low-charge-state high-current case (1  $\mu$ A).

### Magnet System

The "C" type dipoles will allow merged ion-laser beam experiments and easy access to the vacuum chamber. A 7.0-cm dipole vertical gap is required: 4.5 cm for betatron motion and closed-orbit errors and 2.5 cm for beam pipe, bakeout insulation, and shims. The maximum horizontal good field requirements of 12 cm occurs for slow extraction of a full  $40\pi$  mm-mrad beam. Because of the 12.7-cm sagitta, the dipoles will be curved to follow the central trajectory. For simplicity of construction, the magnet

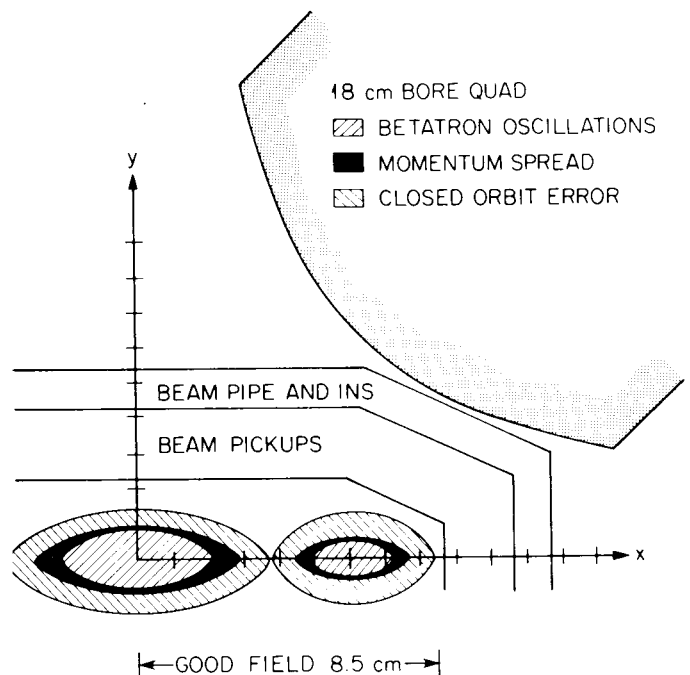


Fig. 5. Aperture requirement in the F quadrupole. The beam centered at +6.0 cm ( $\Delta Q/Q = \pm 4\%$ ) has  $\epsilon = 13\pi$  mm·mrad with  $\Delta P/P = 0.1\%$ . This beam requires a good field at 8.5 cm which in turn determines the bore of 18 cm and pole-tip width of 15 cm. For comparison a central full beam of  $\epsilon = 40\pi$  mm·mrad with  $\Delta P/P = 0.3\%$  is also shown.

quadrupole aperture requirement for this case. The  $\pm 4\%$  charge-state beam centered at  $x = +6.0$  cm has  $\epsilon = 13\pi$  mm·mrad as required. The aperture required for betatron oscillations, momentum spread, and closed-orbit errors is shown. This beam requires a good field radius of 8.5 cm, and a field derivative accuracy of  $\pm 0.05\%$  out to this radius requires a quadrupole with an 18-cm bore. Space for beam pickups, beam pipe, and bakeout insulation is also shown. For illustration, a central beam with  $\epsilon = 40\pi$  mm·mrad with  $\Delta P/P = 0.3\%$  is shown. At the nominal tunes, the quadrupoles require a gradient near 4.2 T/m with an effective length of 50 cm. The quadrupoles will have a cross sectional area of 80 cm x 80 cm, a core length of 42 cm, and will weigh 1.8 tons. Each pole will require a peak current of 165 A in 95 turns. Both the dipole and quadrupole magnets will be constructed from 1.5-mm-thick laminated magnet steel.



The power supply requirements are dominated by the power converter needed to excite the dipoles. This power converter has been sized at 700 kVA, the approximate level used to drive the BNL NSLS booster dipoles. With the eight dipoles connected in series, with the maximum resistive power, and with a 20% safety margin, this 700-kVA supply can drive the inductive load at a rate equivalent to a  $\dot{B}$  of 1.7 T/s. This supply can thus ramp the dipoles from the 0.6-T injection level to the maximum 1.2-T level in 0.35 s. With the assumption of 0.1 s for injection and rf capture and a 50% experimental duty factor, a minimum total cycle time of 1.6 s is estimated. The twelve quadrupoles have been divided into three circuits with 56-kVA power supplies per circuit.

#### RF Acceleration/Deceleration System

The rf system will accelerate and decelerate ions injected from either the tandem or the RFQ linac. The rf cavity voltage required for acceleration, the rf cavity voltage required to capture the beam energy spread, and the rf frequency range all depend on the injection mode, charge-to-mass ratio, kinetic energy per nucleon, and stripping foil configuration. These rf needs were analyzed in terms of the reference ions listed in Table 2. Analysis showed that a peak rf voltage of 2.5 kV/turn is more than adequate for all applications. A frequency range of at least a factor of ten is needed, particularly to decelerate the heaviest ions. To use the same cavity for all applications, the harmonic number must be varied to match the specific case. Ions injected from the tandem and RFQ will normally be accelerated with the first and second harmonics, respectively, whereas deceleration will require much higher harmonics.

A frequency range of a factor of ten requires the use of MnZn ferrite which is noted for its wide permeability range. This ferrite selection restricts the practical tuning range to a maximum frequency of about 2.5 MHz. Cavity parameters which meet these criteria are listed in Table 4. A cavity configuration

Table 4. rf Cavity Characteristics

Tuning range	0.2 to 2.5 MHz
Overall length	1.2 meters
Inner conductor OD	0.3 meters
Outer conductor ID	0.5 meters
Beam tube ID	0.2 meters
Ferrite rings	
Material	MnZn
ID	0.3 meters
OD	0.5 meters
thickness	0.025 meters
number	32
Cooling for ferrite	forced air
Cooling for copper	water
Number of accelerating gaps	2
Peak rf voltage per gap	1250 volts
Total peak rf drive power	3600 watts
Ferrite permeability range	12 to 1800
Peak ferrite bias current	3000 amperes
Peak bias supply voltage	16 volts

was selected which is very similar to the BNL AGS design. This cavity is a full-wave coaxial resonator with accelerating gaps at the one-quarter and three-quarter wave points.<sup>15</sup> A cross-sectional view of the cavity is shown in Fig. 6. The gap voltage requires a ferrite power loss of less than 40 mW/cc allowing air cooling. The ferrite rings will probably be TDK type PE7B which was fabricated for BNL tests. A total of 32 rings with a weight of 552 kg will be needed. The cavity requires about 4 kW of power;

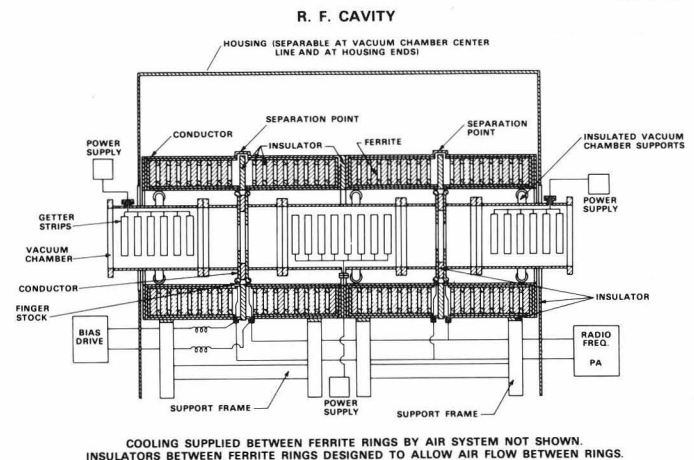


Fig. 6. Cross section of the rf acceleration/deceleration cavity. The frequency will be varied from 0.2 to 2.5 MHz with 500 kg of biased ferrite. A total voltage of 2.5 kV/turn is needed.

therefore, a 10 kW power amplifier will be used after considering the uncertainties in cavity losses, ferrite losses, load mismatch, and voltage requirements.

#### Vacuum System

The vacuum requirement to decelerate and store highly charged very-heavy ion is severe. Heavy ions passing through residual gas can either capture electrons from gas molecules or lose electrons by colliding with gas molecules. Estimates of beam lifetimes in HISTRAP from charge-changing collisions were made using the electron capture cross sections of Schlacter<sup>16</sup> and electron loss cross sections of Alonso and Gould.<sup>17</sup> The vacuum requirements resulting from these calculations for a tandem-injected  $Au^{40+}$  beam, one of the worst cases, is summarized in Fig. 7 which shows the survival fraction as a function of HISTRAP chamber pressure for various operating modes with  $Au^{40+}$  ions beam in a residual gas of 90%  $H_2$  and 10%  $N_2$ . The upper panels are for acceleration from 1.9 MeV/A to 7.9 MeV/A and for deceleration from 1.9 MeV/A to 0.10 MeV/A. The remaining panels are for one-second coasts (one-second storage times) at 7.9, 1.9, 0.10 and 0.02 MeV/A. With a vacuum pressure of  $1 \times 10^{-12}$  Torr, about 50% of a coasting 20 keV/A  $Au^{40+}$  beam would be lost in one second. For acceleration and storage at high energies pressures in the order of  $5 \times 10^{-11}$  Torr are acceptable.

The vacuum system will be designed to eventually reach a base pressure of  $10^{-12}$  Torr. All major components must be fabricated of electropolished 316 LN stainless steel. All stainless components will be vacuum baked at 950°C before assembly. The stainless must have a specific outgassing rate of less than  $10^{-13}$  Torr  $\ell/s/cm^2$ . All components will be designed and tested to withstand a 300°C bakeout in situ for 24 hours. Each octant of the ring will be equipped with an extractor ion gauge, a 60- $\ell/s$  magnetic sputter-ion pump and a titanium sublimator pump. Residual gas analyzers will be made a permanent part of the vacuum system. An experimental vacuum program will be carried out before the final preparation method, chamber materials, and other components are specified.

#### Electron Beam Cooling System

An electron beam cooling system will be used in HISTRAP to reduce the energy spread and angular divergence of ions used for high-resolution spectroscopic studies. In addition, as a practical necessity,

ORNL-DWG 85-18504

### TANDEM INJECTION

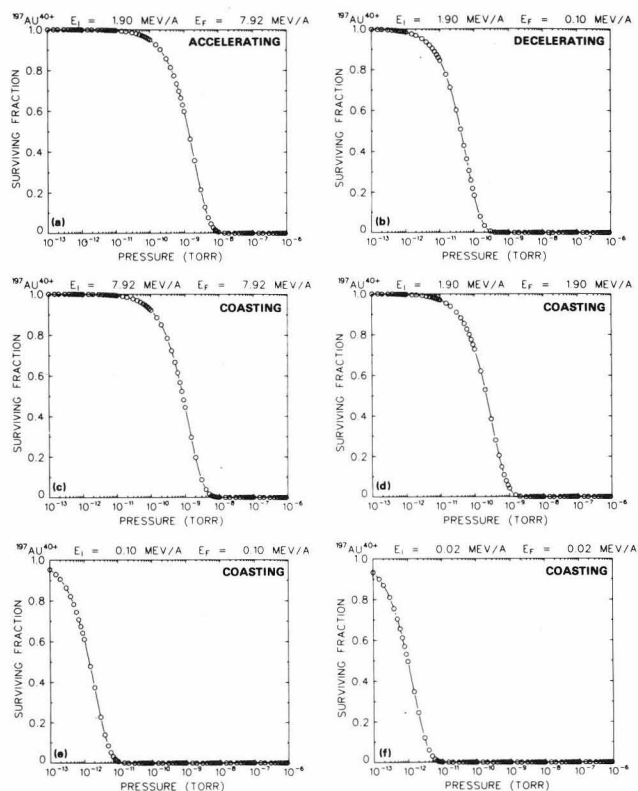


Fig. 7. The surviving fraction for tandem-injected Au beams as a function of vacuum system pressure for various HISTRAP operating modes. The residual gas was assumed to be 90% H<sub>2</sub> and 10%N<sub>2</sub>. E<sub>i</sub> and E<sub>f</sub> are the initial and final kinetic energies per nucleon, respectively.

beam cooling is required prior to deceleration since decreasing the ion velocity will increase the angular divergence and relative energy spread of the beam which in turn will increase the beam size beyond the aperture of the machine. The electron cooling system is shown in Fig. 8 and the corresponding parameters are listed in Table 5.

Table 5. Parameters of the Electron Cooling System

Length of the cooling region	1.00 m
Cathode diameter	5 cm
Electron beam diameter	5 cm
Acceleration	resonant
Deceleration in collector	nonresonant
Electron energy, maximum (minimum)	60 keV (1 keV)
Electron current loss	< 1%
Beam current, maximum (minimum)	5 A (10 mA)
Magnetic field, maximum (minimum)	0.2 T (0.02 T)
Magnetic field stability, ΔB/B	5 × 10 <sup>-5</sup>
High voltage stability, ΔV/V	5 × 10 <sup>-6</sup>
Toroid deflection angle	48 degrees
Toroid bending radius	0.5 m
Magnetic field alignment to the ion axis	< 2 × 10 <sup>-4</sup> rad

The system will consist of three major components immersed in a solenoidal magnetic field: an electron gun, a drift region, and collector. Two identical toroidal magnets will deflect, by 48 degrees, the electron beam in and out of the 1-meter-long drift region where the ion cooling takes place. In order to produce the minimum possible angular divergences and cooling times, the drift region requires a solenoidal magnetic field uniform to 50 ppm in space and time. The electrons will be accelerated with a 60 KV precision high-voltage supply. In the collector the electrons will be decelerated to less than 3 keV which will greatly decrease the power requirements of

ORNL - DWG 85-15501

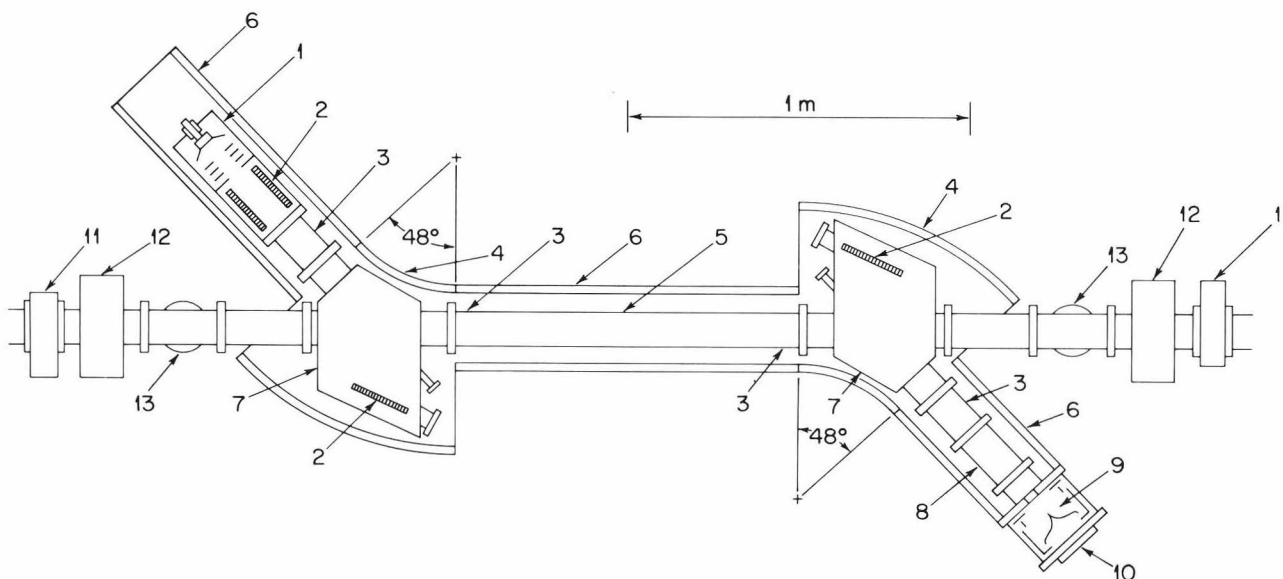


Fig. 8. The electron beam cooling system showing the location of: 1. electron gun, 2. NEG pumps, 3. pick-up station, 4. toroid, 5. central drift tube or interaction region, 6. solenoid, 7. toroid chamber, 8. collector drift tube, 9. collector, 10. pump port, 11. valve, 12. correction dipole, and 13. pumping station.



this supply and also decrease the outgassing problems associated with stopping the intense electron beam. The electron beam cooling system operated with unmatched electron and ion velocities will provide an in-ring experimental device for electron-ion interaction studies.

#### Future Extraction System

The HISTRAP proposal contains no apparatus to extract beam for use in external beam lines. Initially, only in-ring experiments with circulating beams will be performed. However, to allow for future expansion, it is necessary to insure that an extraction system can be accommodated in the ring. Four additional elements are required for a third order resonant slow extraction system: one trim quadrupole to provide fine control of the tune, one extraction sextupole to establish a separatrix and drive the resonance, one electrostatic septum to separate extracted beam from circulating beam; and one magnetic septum to remove the extracted beam from the ring. A simple extraction system in which all these elements are located in a single straight section has been designed. A straight section will be reserved for such a future system.

#### Beam Instrumentation and Controls

The main in-ring beam instrumentation will consist of a horizontal and vertical electrostatic pickup system and at least one beam current transformer. The electrostatic pickups will measure the deviation of the bunched beam from the central orbit and provide correction signals to various feedback control devices. One pickup will be built in each

quadrupole. As shown in Fig. 5, two centimeters of space has been reserved around the beam in the bore of each quadrupole for these pickups. This space largely exists because of the horizontal good-field requirement to hold multiple-charge-state beams and does not require an increased quadrupole aperture.

#### Cost and Schedule

As shown in Fig. 1, the ring will be housed in a new 72' x 58' shielded room to the south of the HHIRF tandem accelerator and to the east of the Atomic Physics and Applications Annex presently under construction. A major 16" water line will be relocated to allow construction of this building. Also as shown in Fig. 1, the 46' x 60' Atomic Physics and Applications Annex will be ideal to house the tandem transfer line and ECR-RFQ injection system. The pro-

posal contains a second floor addition to this annex to house power supplies, a 2 MVA substation for pulsed loads, and a 1 MVA substation for cw loads.

The escalated cost for this project totals \$14.6M spread over a five-year construction schedule. Of the total, \$1.6M (15%) is for engineering design and inspection, \$2.5M (20%) for contingency, and \$10.5 M for construction. About \$1.7M of the construction cost is for buildings and utilities and about \$8.8 M is for accelerator facilities. If funding started in FY 1988, the facility would be ready for atomic physics experiments at the end of FY 1992.

#### References

1. B. Stensgaard, Inst. of Physics, Univ. of Aarhus, private communication.
2. "CRYRING Report," Research Inst. of Physics, Stockholm (March 1985).
3. "Experiments mit Gespeicherten Schwerionen," Memorandum of MPI für Kernphysik Heidelberg (Feb. 1985).
4. A. Noda et al., IEEE Trans. Nucl. Sci. NS-32, 2684 (1985).
5. K. Blasche, D. Böhne, B. Franzke, and H. Prange, IEEE Trans. Nucl. Sci. NS-32, 2657 (1985).
6. R. E. Pollock, IEEE Trans. Nucl. Sci. NS-30, 2056 (1983).
7. A. Johansson and D. Reistad, CELSIUS- Note 84-42, Uppsala (Oct. 1984).
8. "COSY Studie," Jül-Spez-242, Kfa Jülich (Feb. 1984).
9. J. B. Ball, IEEE Trans. Nucl. Sci. NS-30, 1363 (1983); C. M. Jones et al., Nucl. Instrum. Methods, Phys. Res. A244, 7 (1986).
10. G. D. Alton and C. M. Jones, Nucl. Instrum. Methods, Phys. Res. A244, 170 (1986).
11. G. D. Alton, Nucl. Instrum. Methods, Phys. Res. A244, 133 (1986).
12. F. W. Meyer, Nucl. Instrum. Methods, Phys. Res. B9, 532 (1985).
13. R. A. Gough et al., IEEE Nucl. Sci. NS-32, 3205 (1985); S. T. Staples et al., IEEE Nucl. Sci. NS-32, 3208 (1985).
14. J. Galayda et al., IEEE Trans. Nucl. Sci. NS-26, 3919 (1979).
15. M. Plotkin, private communication (1986).
16. Alfred S. Schlachter, Tenth International Conference on Cyclotrons and Their Applications, MSU, 29 April-3 May, 1984, ed. F. Marti, IEEE Catalog No. 84 CH1996-3, pp. 563-70.
17. J. Alonso and H. Gould, Phys. Rev. A 26, 1134 (1982).